Chapter 5

Design of PSS Using NARMA-L2 and GA-ANN Controller with TCSC

5.1 Introduction

The power system stabilizer has been designed using Non Linear Autoregressive Moving Average-L2 controller and hybrid Genetic Algorithm based Network Network. In order to achieve appreciable damping, developed ANFIS based Thyristor control series capacitor has been suggested in addition to power system stabilizer. The non-linear simulations of single machine infinite bus system (SMIB) have been carried out using individual and simultaneous application of PSS and TCSC. Trained and optimized NARMA-L2 and GA-ANN based PSS have been tested with ANFIS-TCSC on non-linear power system dynamics under the different operating conditions, various disturbances and faults in the power system. The results have shown efficacy and capability of proposed control schemes under the various operating conditions and faults, and demonstrate the improvement in the dynamic performance of the system with proposed control algorithm.

5.2 Nonlinear Auto regressive Moving average -L2 Controller

Nowadays, artificial neural network controllers have been effectively introduced to improve the performance of nonlinear control systems. Unlike conventional controllers, no exact mathematical model is required for ANN controller, and it shows better results in terms of time response parameters such that settling time, delay time, overshoot and robustness. There are several approaches to neural network training [87] for determining an appropriate set of weights. The neural network based identification techniques successfully can be applied for non linear control problem as reported by [87][42].

5.2.1 NARMA-L2 (Feedback Linearization) Control

NARMA-L2 controller has been successfully applied for the identification and controller design. The execution of NARMA-L2 controller involves typically two stages. First stage is identification, which includes development of neural network model of the plant to be controlled. Second stage is controller design, in which training of neural network controller is carried out using developed neural network plant model. The identified NN plant model is used in neural network controller that transforms the non linear system into linear system through additive and multiplicative cancellation of nonlinearities.

5.2.1.1 Identification Stage

The first stage of plant identification process is to generate input/output data pairs to train a neural network to represent the forward dynamics of the plant. The system identification stage has been represented by Figure 5.1. There are two sets of inputs to the plant model, one is delayed values of the plant output and other is delayed values of the controller output.

The model used for the plant identification is described as follow:

$$y(k+d) = N\left[y(k), y(k-1)\ldots\ldots y(k-n+1), u(k), u(k-1)\ldots\ldots u(k-n+1)\right] \quad (5.1)$$

Where $u(k)$ is the system input, $y(k)$ is the system output, and d is system delay. During the identification stage, the neural network training is realized in order to approximate the nonlinear function N. If the system follows a desired reference trajectory y_r, then the nonlinear controller can be written as follow:

$$u(k) = G\left[y(k), y(k-1)\ldots\ldots y(k-n+1), y_r(k+d), u(k), u(k-1)\ldots\ldots u(k-m+1)\right] \quad (5.2)$$

The neural network training could be performed to determine the function G that minimizes the mean square error using back propagation training algorithm. The dynamic of back propagation is slow and computationally demanding. To achieve faster response [19, 9, 87] proposed the use of NARMA-L2 controller approximate model in companion form and is represented as equation (5.3).

$$\hat{y}(k+d) = f\left[y(k), y(k-1)\ldots\ldots y(k-n+1), u(k-1)\ldots\ldots u(k-m+1)\right] +$$

$$g\left[y(k), y(k-1)\ldots\ldots y(k-n+1), u(k-1)\ldots\ldots u(k-m+1)\right].u(k) \quad (5.3)$$

Here the next controller input $u(k)$ is not contained in the nonlinearity. The advantage of this form is that user can solve for the control input that causes the system output to follow the reference $y(k+d)$ $=y_r(k+d)$. The resulting controller would have the form as described by equation (5.4).

$$u(r) = \frac{y_r(k+d) - f\left[y(k), y(k-1)\ldots\ldots y(k-n+1), u(k-1)\ldots\ldots u(k-m+1)\right]}{g\left[y(k), y(k-1)\ldots\ldots y(k-n+1), u(k-1)\ldots\ldots u(k-m+1)\right].} \quad (5.4)$$

Using this equation directly can cause realization problems; the determination of the control input based on the output at the same time is not realistic and hence uses the following model:

$$y(k+d) = f\left[y(k)\ldots\ldots y(k-n+1), u(k)\ldots\ldots u(k-n+1)\right] +$$

$$g\left[y(k)\ldots\ldots y(k-n+1), u(k)\ldots\ldots u(k-n+1)\right].u(k+1) \quad (5.5)$$

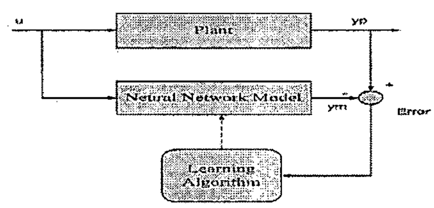

Figure 5.1: Identification Stage

5.2.1.2 Controller Stage

A more practical form of controller is given by (5.6). This controller is realizable for $d \geq 2$. The controller structure [9] has been shown in Figure 5.2.

$$u(k+1) = \frac{y_r(k+d) - f\left[y(k)\ldots\ldots y(k-n+1), u(k)\ldots\ldots u(k-n+1)\right]}{g\left[y(k)\ldots\ldots y(k-n+1), u(k)\ldots\ldots u(k-n+1)\right].} \tag{5.6}$$

$$\Delta V_{pss}(k+1) = \frac{\Delta\omega_r(k+2) - F}{G} \tag{5.7}$$

Where,

$F = G = f\left[\Delta\omega_m(k), \Delta\omega_m(k-1), \Delta\omega_m(k-2), \Delta V_{pss}(k), \Delta V_{pss}(k-1), \Delta V_{pss}(k-2)\right]$

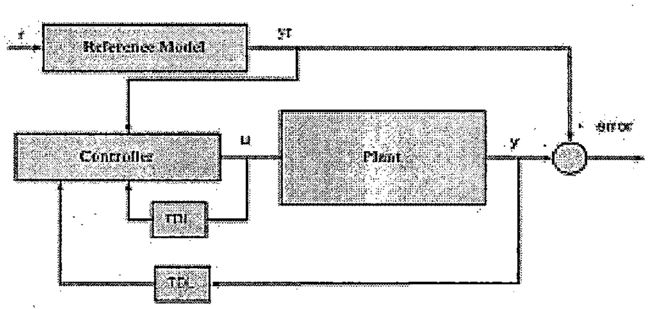

Figure 5.2: NARMA-L2 Controller

5.3 NARMA-L2 Controller based Power System Stabilizer

An indirect data based approach has been used for approximate linearization through feedback. Indirect data base technique is two step methodology, where a model of the plant is identified on the basis of input output data and then used in model based design of a suitable controller.

5.3.1 Neural Network Identifier

NARMA-L2 neural controller has been proposed for the designing of the PSS for power system stability improvement. The identification of neural network base plant is developed using non linear auto regressive moving average model. For the particular system y, u and $\hat{y}$ are the speed deviation $\Delta\omega_m(k)$ of the plant, output of the neural network controller $\Delta V_{pss}(k)$, and predicated plant output $\Delta\hat{\omega}_m(k)$ by the neural network identifier respectively. The training process of the neural network identifier has been shown in Figure 5.3.

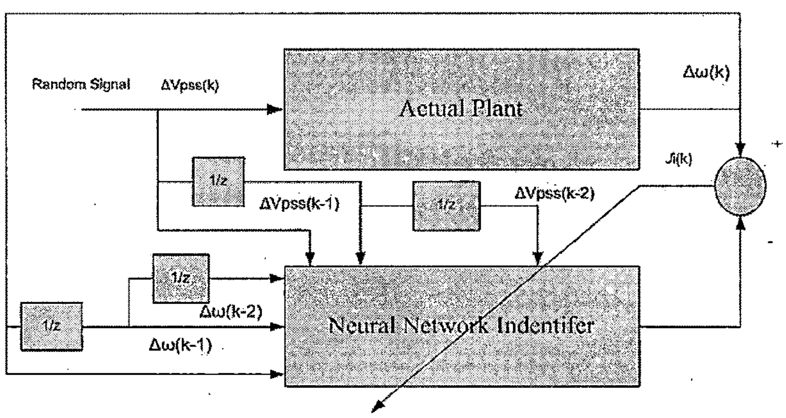

Figure 5.3: Identification of the Plant

Random inputs have been applied to the plant model to generate the input output data. The values of random signal are distributed between -0.04 to 0.04, which are taken from CPSS simulation. Here, 10000 data are used for the identification of the plant. The neural network plant model has two inputs available namely delayed controller outputs and delayed plant outputs. The inputs to the neural network identifier during this phase are $\Delta\omega_m(k), \Delta\omega_m(k-1), , \Delta\omega_m(k-2), \Delta V_{pss}(k), \Delta V_{pss}(k-1), \Delta V_{pss}(k-2)$. The optimization function of the neural network identifier is given by equation (5.8). Where $\Delta\hat{\omega}_m(k)$ is NN identifier output.

$$J_i(k) = \frac{1}{2}\left[\Delta\omega_m(k) - \Delta\hat{\omega}_m(k)\right]^2 \tag{5.8}$$

The neural network identifier is a multilayer feedforward network which is trained by the Levenberge-Marquardt algorithm as described by Section (4.4.1). The feedforward network has been developed with 10 neurons in hidden layer and 1 neuron in output layer with hyperbolic tangent sigmoid and linear transfer functions in first layer and hidden layer, and output layer respectively. Figure 5.4 shows input data to the plant, actual plant output, NN plant output and error between actual plant output and NN plant output. The NN trained plant model is similar to actual plant and error is varied between -0.00004 to 0.00004 rad/sec.

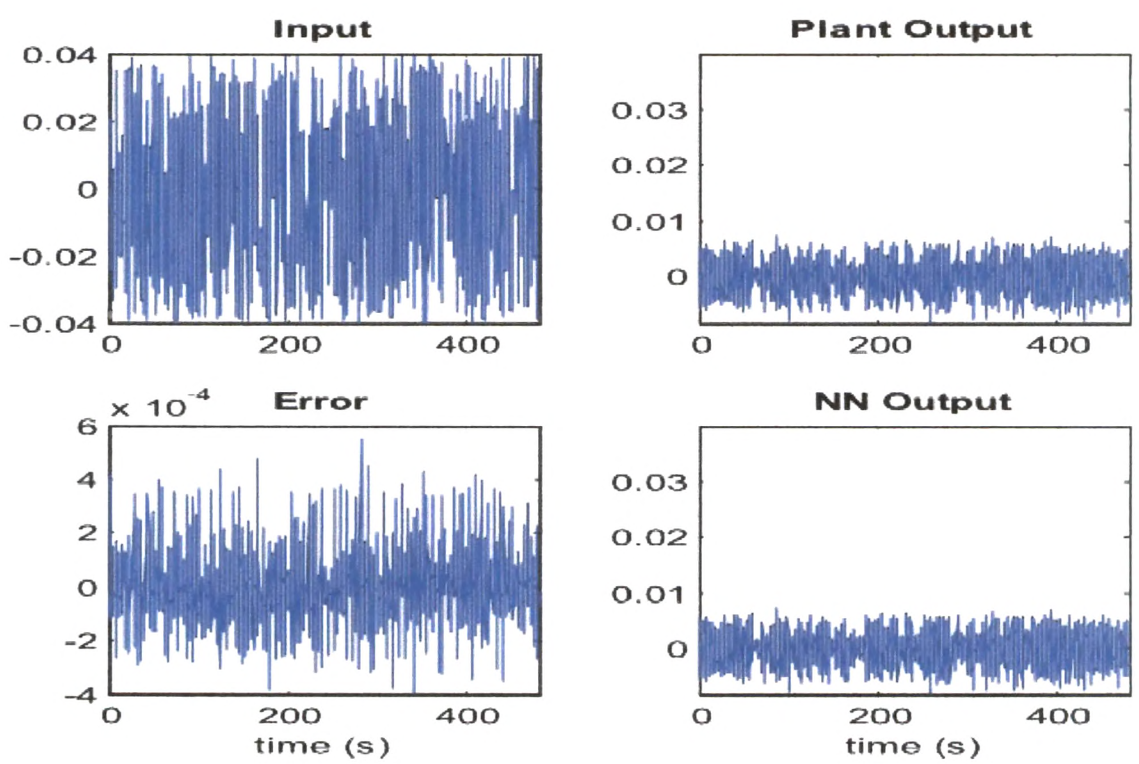

Figure 5.4: Plant Input, Plant Output, NN Output and Error

5.3.2 Neural Network Controller

The neural network controller has been implemented with the identified neural network plant model. The central idea of this controller is to transform nonlinear system dynamics by cancelling the nonlinearities. The neural network controller is also trained by the Levenberge-Marquardt algorithm with 10 neurons in hidden layer. The controller structure has been shown in Figure 5.5 and the controller can be written by the following equation.

$$\Delta V_{pss}(k+1) = \frac{(\Delta\omega_r(k+2) - F)}{G} \tag{5.9}$$

Where,

$F = G = \Delta\omega_m(k), \Delta\omega_m(k-1), , \Delta\omega_m(k-2), \Delta V_{pss}(k), \Delta V_{pss}(k-1), \Delta V_{pss}(k-2)$

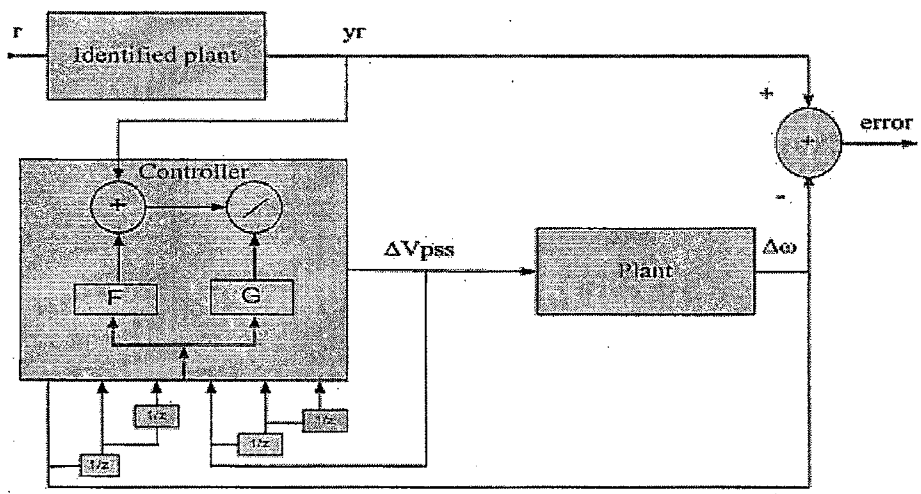

Figure 5.5: Implementation of NARMA-L2 Controller

5.4 GA-ANN Hybrid-Power System Stabilizer

Genetic Algorithm and Artificial Neural Network in the broad sense, reside in the class of the evolutionary computing algorithm. Both GAs and ANNs are adapting, they learn, and can deal with high non linear, complex model. The objective of the hybridization is to overcome the weakness in one technology during its application, with the strengths of the other by appropriately integrating them.

In this section, design of power system stabilizer using combination of genetic algorithm based neural network hybrid controller [94, 89] for analysis of dynamical power system has been discussed. Two different strategies have been used for designing of neural network through GA. In the first strategy, a genetic algorithm has been used to minimize the error before learning algorithm is applied and for second strategy, a genetic algorithm has been used to minimize the sum of square of error with respect to the ANN parameters [94]. Here, the calculation of weight and bias of ANN have been considered as an optimization problem. The weights and bias of the feed forward neural network have been identified and optimized using genetic algorithm. The trained and optimized GA-ANN based PSS has been tested on non-linear power system dynamics under the different operating conditions, various disturbances and faults in the power system.

5.4.1 Genetic Algorithm

Genetic algorithm has been proposed to calculate the initial values of parameters of neural network, the algorithm as follows:

1. Randomly generate the initial population for the parameter of initial weight and bias of NN.

2. Calculation of total number of weight and bias of NN for optimization.

3. Generate the fitness function to be evaluated.

4. Evaluate fitness function of each chromosome in population and select a new population from old population based on the fitness of individuals as given by the evaluation function.

5. Selection of appropriate value of genetic operators such as reproduction, crossover, mutation etc. to member of the population to create new solution.

6. Calculation of convergence rate of fitness function.

7. If expected convergence rate is achieved then stop the algorithm otherwise repeat from the step 4-7 and change the GA parameters.

By changing the GA parameters such as population size, crossover rate and function, mutation rate and function, No. of generation etc, the new set of NN parameters are developed, and best fitness values have been selected. The appropriate choice of the GAs parameters affects the convergence rate of the algorithm. The parameters are selected for expected solution as given in Table 5.1. Figure 5.6 shows the rate of the convergence of the optimization function, the best fitness value of the function 0.00021793 is achieved after the 51 generation has been reached. Figure 5.7 shows the total 81 best individual values of weight and bias of NN.

Table 5.1: GA Parameter and Value

Parameters	Values/Parameter
Popullation Size	50
Stopping Generation	100
Scaling Function	rank
Selection Function	Stochastic Uniform
Mutation Function	Gaussian
Crossover Function	Scattered

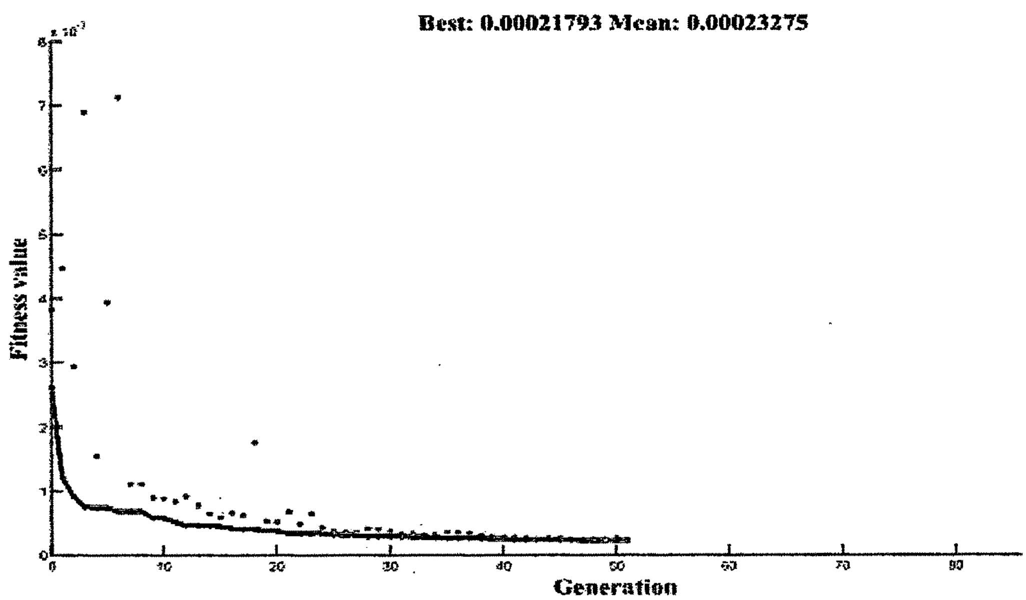

Figure 5.6: Convergence rate of GA

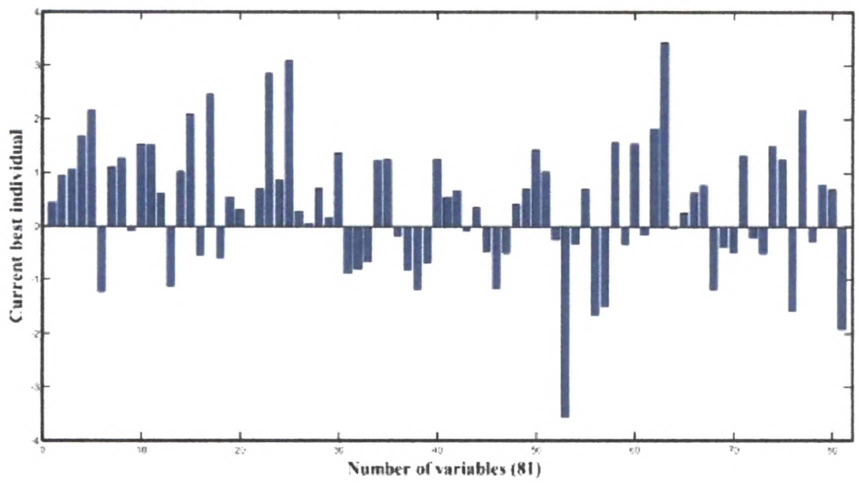

Figure 5.7: Best Value of NN Parameters

5.4.2 Neural Network

The training pattern for the feedfoward neural network is dynamic inputs $u(t)$ and corresponding outputs $y(t)$ such that $\omega_m(t), \omega_m(t-1), \omega_m(t-2), \omega_m(t-3)$ and V_{pss} respectively and targeted value of the neural network is $\hat{y}(t)$. The network has been trained using 8000 sample data, which are generated under the consideration of the different operating conditions and dynamic behavior of the power system. The feedforward network has been developed with 10 neurons in the first layer, 5 neurons in hidden layer and 1 neuron in output layer with hyperbolic tangent sigmoid transfer function between first layer and hidden layer, and linear transfer function between hidden layer and output layer. In this problem, derivative -based optimization Levenberg-Marquardt method is used for solving the nonlinear least squares problem.

The weights and bias of the network are adjusted such that the error between the actual output and targeted output is minimized and desired goal is achieved through Levenberg-Marquardt derivatives -based optimization. The optimization function can be represented mathematically by equation (5.10). Levenberg-Marquardt's direction [87, 14] that is determined by using equation (4.13) is an intermediate between the Gauss-Newton direction and the steepest descent direction. The optimization function can be represented by Equation

$$J_i(k) = \frac{1}{2}\Sigma \left[y(k) - \hat{y}(k)\right]^2 \tag{5.10}$$

The Gauss Newton Levenberg-Marquardt method works well in practice and has become standard of nonlinear least squares routines [87, 14].

The following steps are for implementation of neural network

1. The initial parameters of NN likes weights and bias are computed by GA.

2. Generate the input data pattern and corresponding the target data pattern.

3. Develop the feedforward neural net.

4. Train the neural network using Levengerg-Marquardt algorithm[14].

5. Update the NN parameters through equation of Levenberg-Marquardt Algorithm.

6. Calculation of mean square error between actual output and targeted output using Equation (5.10)

7. Compute the output of the NN network

8. If desired solution is achieved stop, else change the NN goal, learning rate, no. of epochs and repeat the algorithm from the step 4.

Figure 5.8 shows the error generated between actual data and target data and Figure 5.9 shows the relation between training data versus actual data and target data.

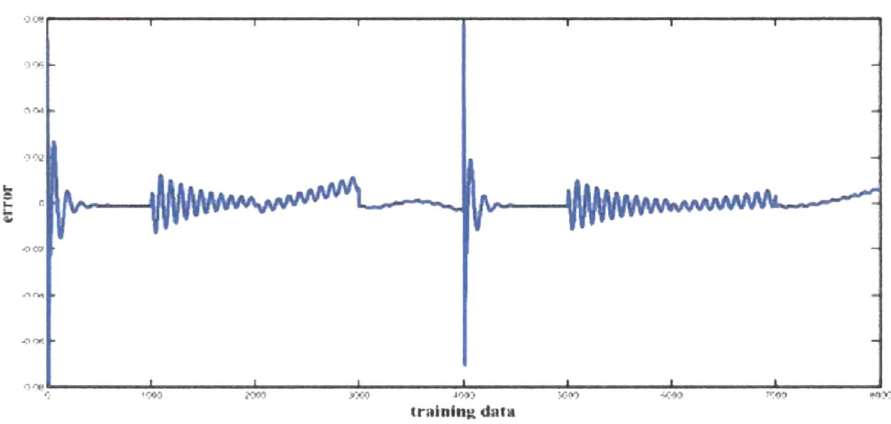

Figure 5.8: Error Between Actual and Target Value

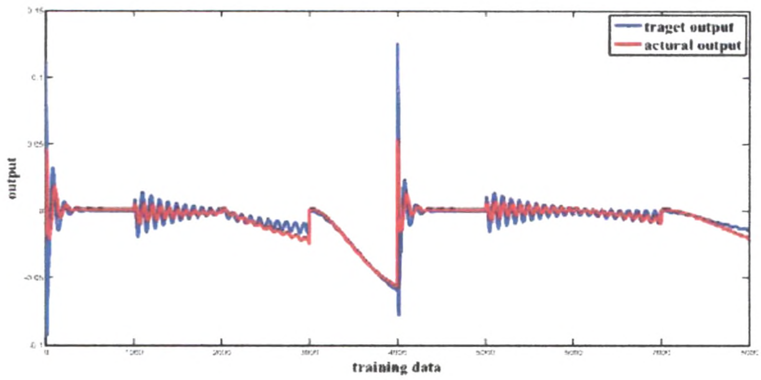

Figure 5.9: Output of GANN

5.5 Non Linear Simulation

The nonlinear model of the power system has been used for the stability analysis of the SMIB system with generator attached PSS and transmission line connected TCSC. The initial conditions of power system have been calculated using MATLAB programming. The non-linear simulation is carried out using non-linear dynamic model, which has been implemented using MATLAB/simulink environment. The non linear model and detailed data of the power system used in this study is given by Appendix A. The comparison analysis between (i) NARMA-L2 Controller and GA-ANN based PSS (ii) simultaneous application of ANFIS-TCSC with NARMA-L2-PSS and GA-ANN-PSS have been carried out under different operating condition, faults and disturbance. These disturbances considered are such as the three phase short circuit at the infinite bus, outage of transmission line, suddenly changes in mechanical input and step change in terminal voltage reference. The comparison study of smart techniques based TCSC and PSS has been carried out.

5.5.1 Case I

Considering operating condition 1 as defined in table 3.1 $P_t = 0.6, Q_t = 0.0224$. A three phase fault is created at 1s at the sending end of one the circuits of the transmission line and cleared after 100ms [33]. The original system restored after fault clearance. The response of speed deviation with the application of individual PSS, and simultaneous application of PSS with ANFIS controller has been shown by Figure 5.10 and 5.11 respectively. Figures 3.6 shows that without application of controllers the oscillation in speed deviation are observed while using simultaneous application of ANFIS-TCSC with NARMA-L2-PSS and GA-ANN-PSS have significantly diminished this oscillation in the system and provided very good damping characteristics.

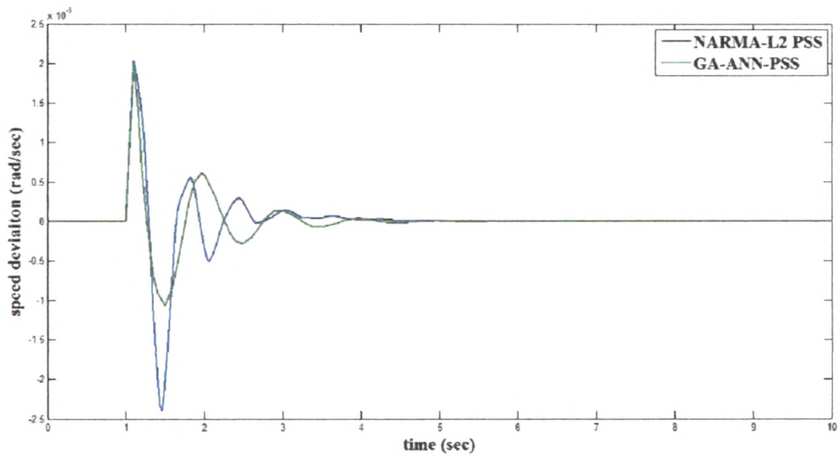

Figure 5.10: Case I: Speed response of NARMA-L2 and GA-ANN based PSS

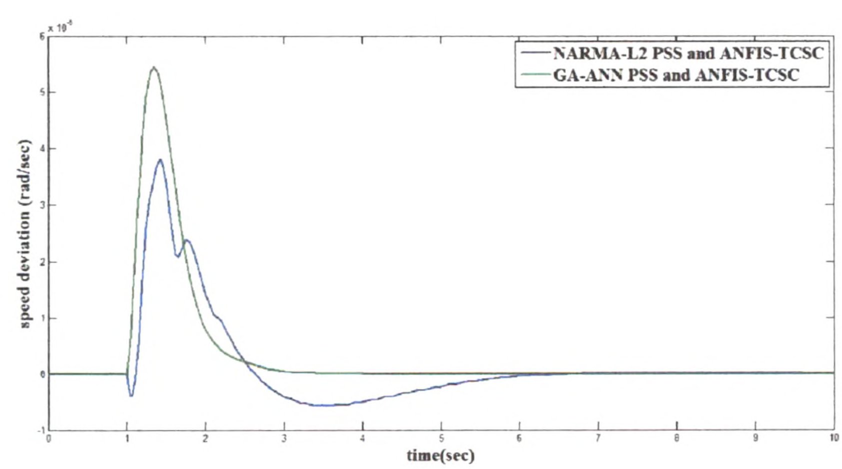

Figure 5.11: Case I: Speed response of NARMA-L2 and GA-ANN based PSS and ANFIS-TCSC

5.5.2 Case II

$P_t = 0.6, Q_t = 0.0224$, A three phase fault is created at 1s at the middle of one transmission line and cleared after 50 ms by the disconnection of the faulted line, and then successfully reclosed at 5s [71]. Figure 3.15 shows the response of the rotor speed deviation without controllers. The response of the ω_m with presence of NARMA-L2-PSS and GA-ANN-PSS has been shown in Figure 5.12. Figure 5.13 shows the response of ω_m with simultaneous application of ANFIS-TCSC and PSS. Without application of damping controllers, the oscillations in speed deviation have been observed. These oscillation are continuous growing, which shows instability of system after 10s. While using individual PSS and simultaneous application of ANFIS-TCSC and PSS have significantly diminished this oscillations and improved stability of the system.

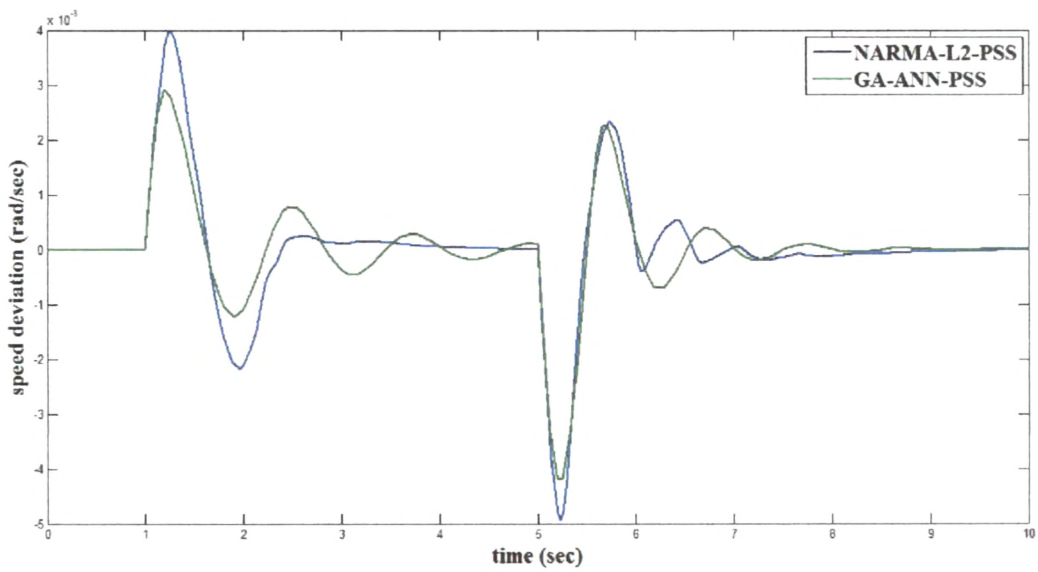

Figure 5.12: Case II: Speed response of NARMA-L2 and GA-ANN based PSS

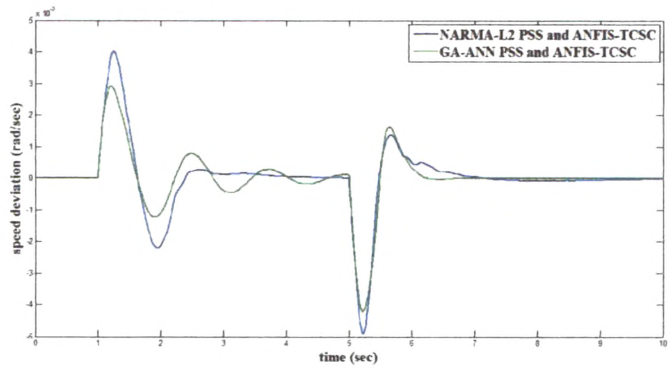

Figure 5.13: Case II: Speed response of NARMA-L2 and GA-ANN based PSS and ANFIS-TCSC

5.5.3 Case III

$P_t = 0.9, Q_t = 0.12$, Here heavy loading condition is considered. A three phase fault is created at 1s at the sending end of one of the circuits of the transmission line and cleared after 50ms. The original system restored after the fault clearance. Figure 3.22 shows the response of the $\omega_m(t)$ without controller, the oscillation in the power system continuously growing with respect to the time and system has become unstable. The speed response with NARMA-L2-PSS and GA-ANN based PSS, and simultaneously application of ANFIS- TCSC with NARMA-L2-PSS and GA-ANN-PSS has been shown in Figure 5.14 and 5.15 respectively. The simultaneous application of ANFIS-TCSC and PSS, and individual applications of PSS reduced the oscillations in the system and improved stability.

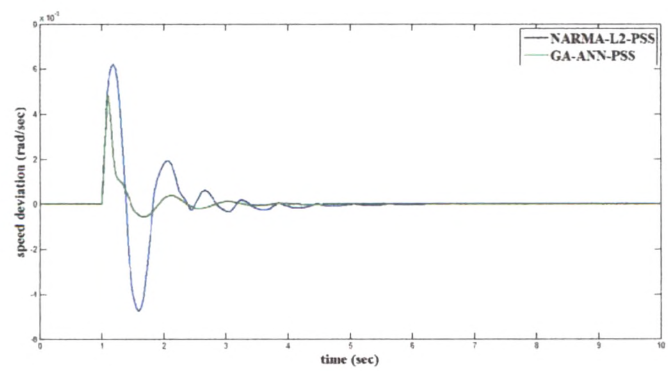

Figure 5.14: Case III: Speed response of NARMA-L2 and GA-ANN based PSS

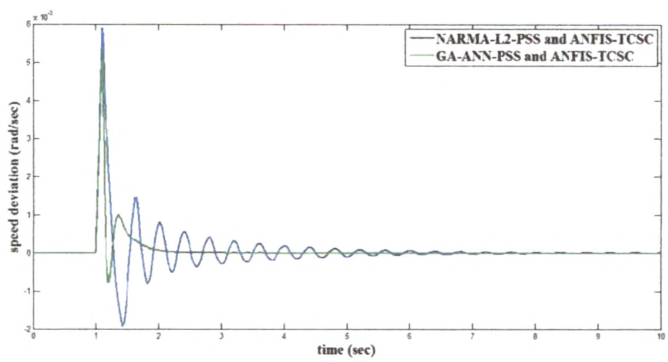

Figure 5.15: Case III: Speed response of NARMA-L2 and GA-ANN based PSS and ANFIS-TCSC

5.5.4 Case IV

$P_t = 0.9, Q_t = 0.12$,Under the heavy loading condition a 10% mechanical change applied at 1s and removed at 5 s is considered. The system lost its stability at 4s without application of controllers, which has been shown by Figure 3.26. Figure 5.16 shows the response of ω_m with individual and simultaneous application of PSS and TCSC. The simultaneous application of TCSC and PSS, and individual applications of PSS reduced the oscillations in the system and improved stability.

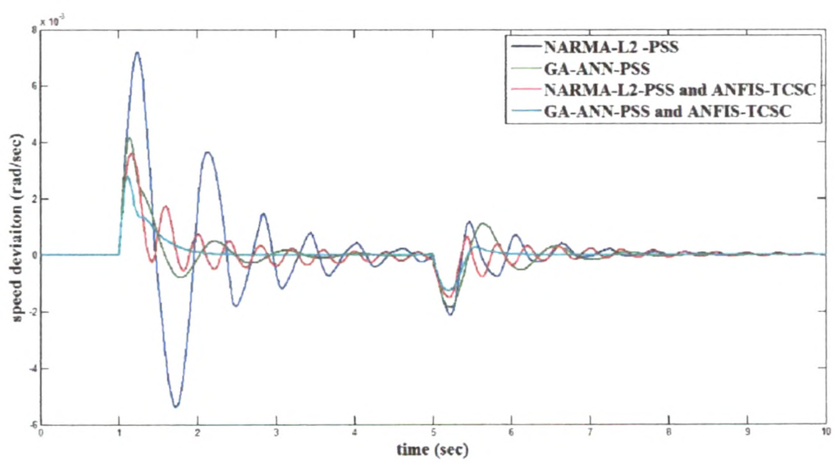

Figure 5.16: Case IV: Speed response of NARMA-L2 and GA-ANN based PSS and ANFIS-TCSC

5.5.5 Case V

$P_t = 1.2, Q_t = 0.2$, A 0.1p.u. change in reference input voltage is applied at 1 s and removed at 5 s. The response of the ω_m without and with presence of controllers has been shown in Figure 3.30 and 5.17 respectively. Figure 5.17 shows that GA-ANN-PSS has been produced better response than NARMA-L2-PSS. Simultaneous application of GA-ANN-PSS and ANFIS-TCSC have been produced best response compared to other controllers

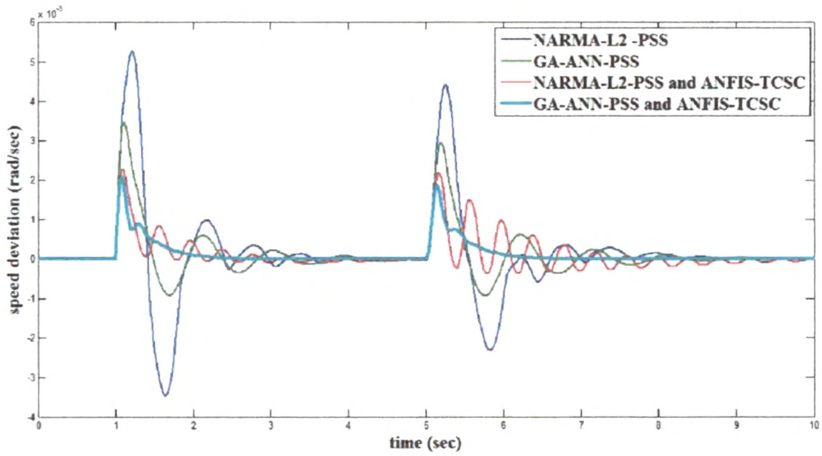

Figure 5.17: Case V: Speed response of NARMA-L2 and GA-ANN based PSS and ANFIS-TCSC

5.5.6 Case VI

$P_t = 0.75, Q_t = 0.1$, In this case another severe disturbance is considered. One of the transmission lines is permanently tripped at 1 sec. The line reactance is significantly increased. The speed response for the above contingency has been shown in Figure 3.34 and 5.18 without and with controller respectively.

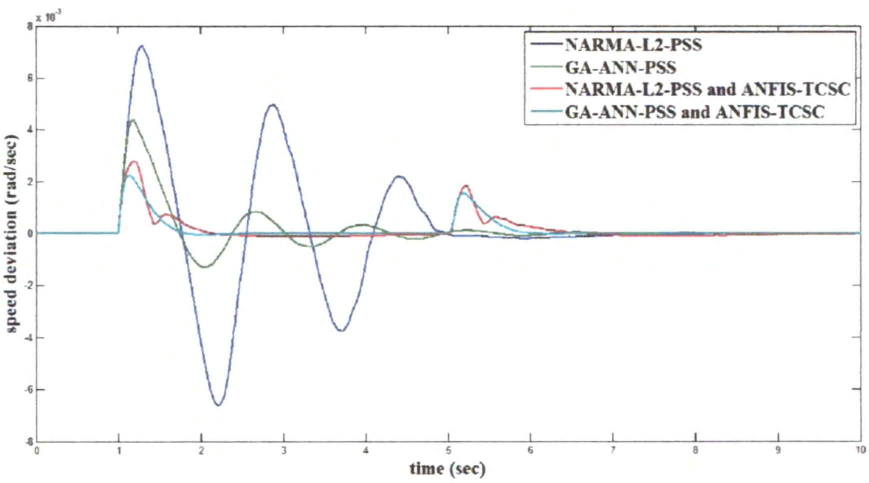

Figure 5.18: Case VI: Speed response of NARMA-L2 and GA-ANN based PSS and ANFIS-TCSC

5.6 Simulation of System with Intelligent Techniques based PSS and ANFIS-TCSC

Here five different types of intelligent controllers based PSSs have been tested under the heavy loading condition. For case I to case III, the operating condition $P_t = 1.2, Q_t = 0.2$ and for case IV the operating condition $P_t = 0.75, Q_t = 0.1$ have been selected for performance assessment of GA-CPSS, LMNN-PSS, ANFIS-PSS, NARMA-L2-PSS and GA-ANN-PSS with dynamic power system under different contingencies. For various cases, all intelligent techniques based PSS are tested with ANFIS-TCSC. The ANFIS-TCSC has been selected because its performance is better than compared to the GA-TCSC and LMNN-TCSC. ANFIS-TCSC has not required to tune for each and every operating conditions like GA-TCSC hence ANFIS-TCSC is better choice for simultaneous application with PSS.

5.6.1 Case I

$P_t = 1.2, Q_t = 0.2$,A 10% mechanical change applied at 1s and removed at 5 s is considered. The speed response with five different types of intelligent techniques based PSS has been shown in Figure 5.19. Figure 5.20 shows all the intelligent PSS applied with ANFIS-TCSC.

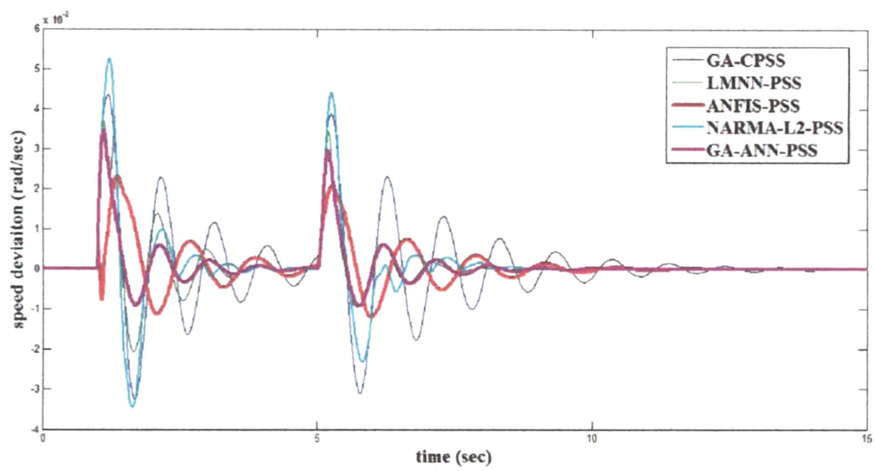

Figure 5.19: Case I: All Intelligent Techniques based PSS

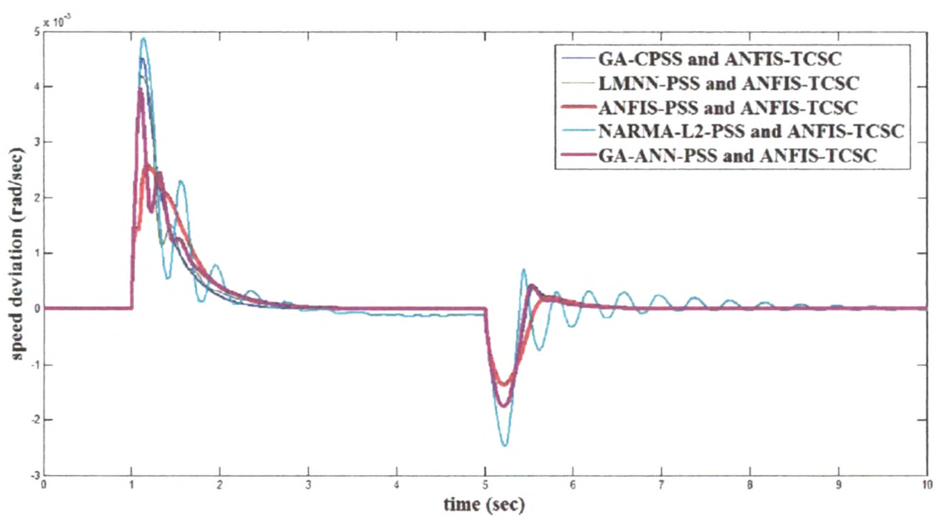

Figure 5.20: Case I: ANFIS-TCSC with Intelligent Techniques based PSS

5.6.2 Case II

$P_t = 1.2, Q_t = 0.2$, A 0.1p.u. change in reference input voltage is applied at 1 s and removed at 5 s. The speed response with five different types of intelligent techniques based PSS has been shown in Figure 5.21. Figure 5.22 shows all the intelligent techniques based PSS applied with ANFIS-TCSC.

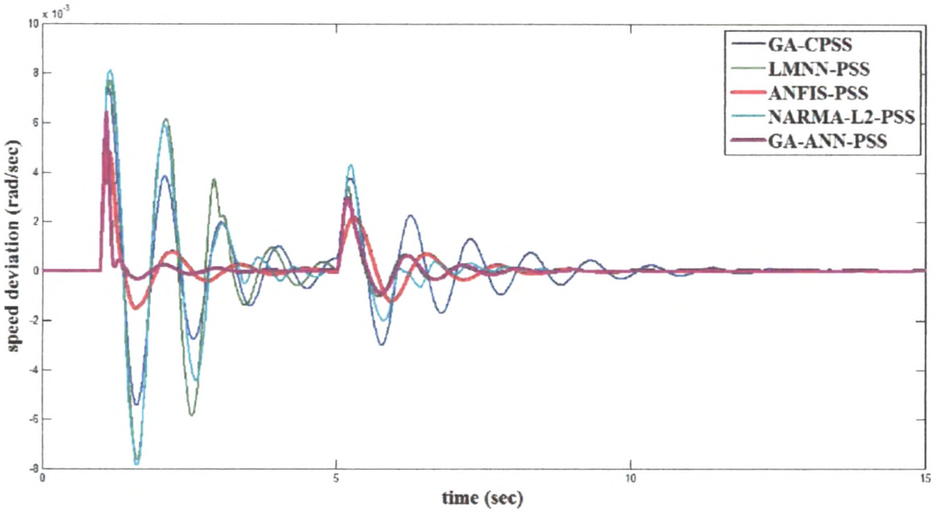

Figure 5.21: Case II: All Intelligent Techniques based PSS

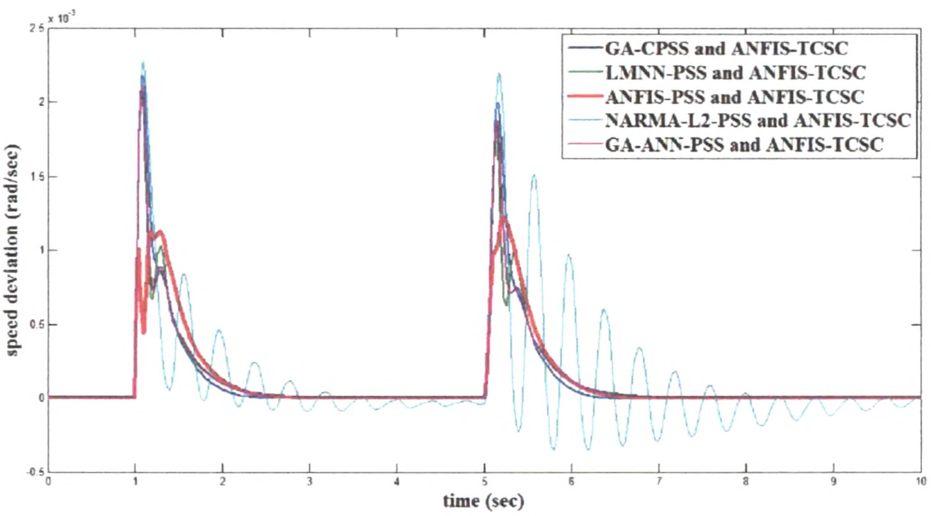

Figure 5.22: Case II: ANFIS-TCSC with Intelligent Techniques based PSS

5.6.3 Case III

$P_t = 1.2, Q_t = 0.2$, A three phase fault is created at 1 s at the sending end of one of the circuits of the transmission line and cleared after 100ms. The speed response with five different types of intelligent techniques based PSS has been shown in Figure 5.23. Figure 5.24 shows the all intelligent techniques based PSS applied with ANFIS-TCSC.

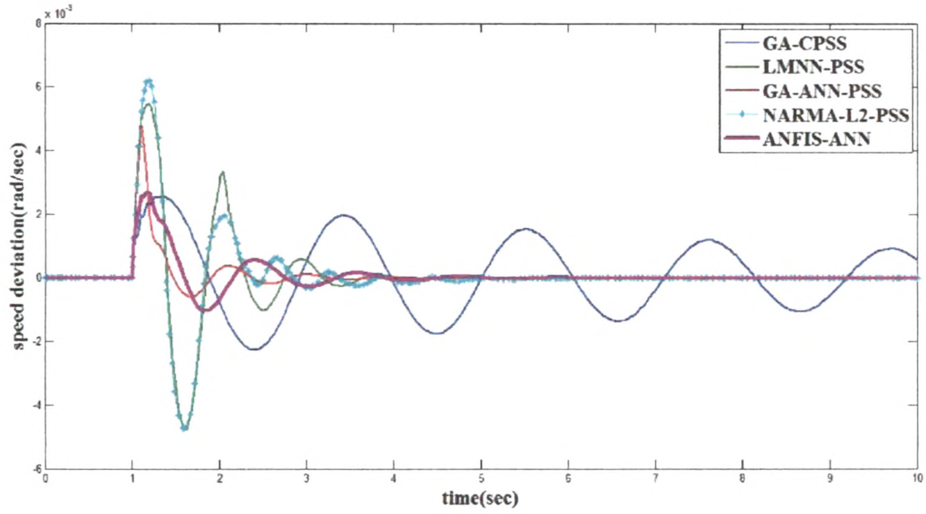

Figure 5.23: Case III: All Intelligent Techniques based PSS

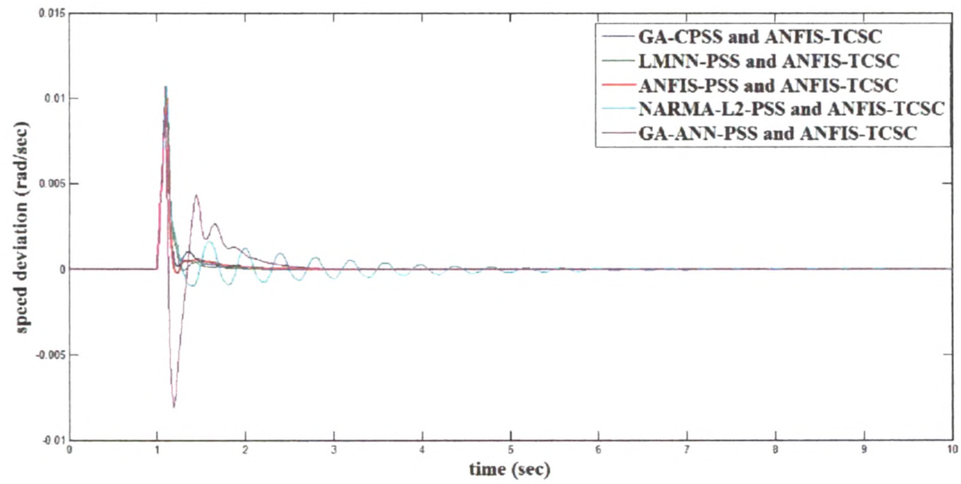

Figure 5.24: Case III: ANFIS-TCSC with Intelligent Techniques based PSS

5.6.4 Case IV:

$P_t = 0.75, Q_t = 0.1$, A fault is created at 1 s at the middle of one transmission line and cleared after 50ms by disconnection of the faulted line, then successfully reclosed at 5s. Figure 5.25 shows the speed response with five different types of intelligent techniques based PSS. All intelligent techniques based PSS applied with ANFIS-TCSC has been shown in Figure 5.26.

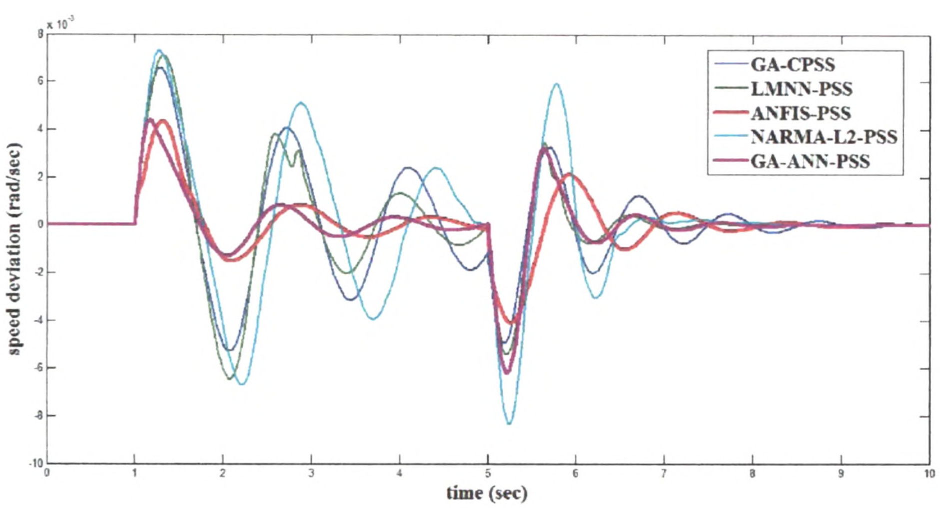

Figure 5.25: Case IV: All Intelligent Techniques based PSS

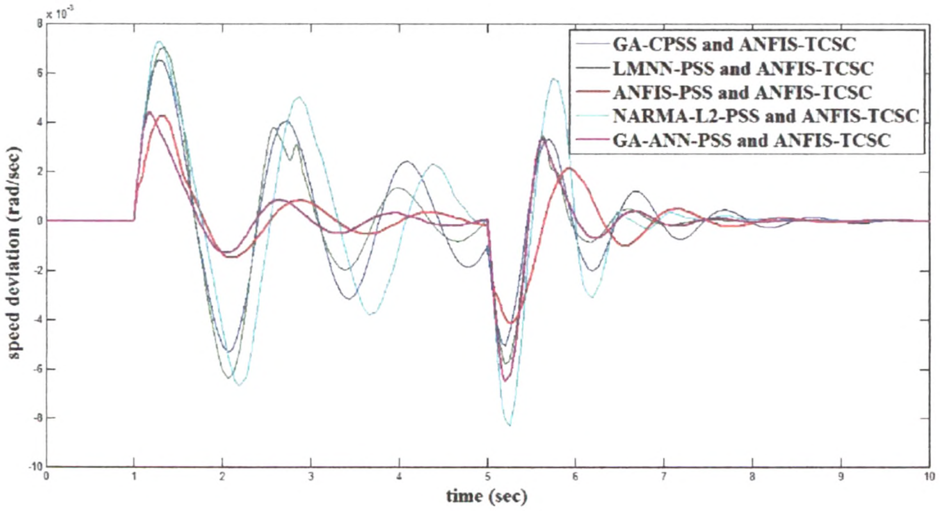

Figure 5.26: Case IV: ANFIS-TCSC with Intelligent Techniques based PSS

5.7 Conclusion

In this study, the smart control strategies based TCSC damping controller and PSS have been designed. The NARMA-L2 and GA-ANN based PSS, and simultaneously ANFIS-TCSC and PSS have been applied to the dynamical power system. The non-linear simulations have been carried out for detailed analysis of the stability of the power system. The time responses of speed deviation obtained by intelligent techniques based controller have been compared to the conventional power system stabilizer. Four different operating conditions are taken and the response of rotor speed deviation has been analyzed under different types of the disturbances and faults.

From the non - linear analysis,

1. Without the application of the controllers in the system, the oscillations in rotor speed deviation has been observed. Under the heavy loading condition, it has been observed that the active power and reactive power are increased; the oscillation in speed deviation is continuously growing which creates the instability of the system. The smart damping controllers have been greatly diminished oscillations in system.

2. Convention power system stabilizer doesn't produce satisfactory response under the different operating conditions. While simultaneous application of ANFIS -TCSC and PSS have provided very good damping characteristics compared to the individual application of PSS and almost eliminated the oscillations in system.

3. Figures have shown that individual application of GA-ANN-PSS produces better response compare to the individual NARMA-L2-PSS.

4. Under the different loading conditions, It has been observed that simultaneous application of GA-ANN-PSS and ANFIS-TCSC produce better response compared to the simultaneous application of NARMA-L2-PSS and ANFIS-TCSC. It improved the time response parameters such as settling time, rise time and delay time appreciably and decreased the overshoot in the system.

In section (5.6), different Intelligent techniques based PSS are tested under heavy loading conditions. Simultaneous ANFIS-TCSC with all PSS are also tested under heavy loading conditions. Following results are obtained from detailed study:

1. The GA-CPSS, ANFIS-ANN and GA-ANN are produced better response compared to the LMNN-PSS and NARMA-L2-PSS.

2. But GA-CPSS required different optimized parameters under different operating conditions and GA-ANN has needed more time for training of neural network. While ANFIS-PSS has been produced fast, adaptive and satisfactory response with less number of training data.

3. From figures (5.19) to (5.26), it has been observed that the ANFIS-TCSC produces better response with GA-CPSS, ANFIS-PSS and GA-ANN-PSS compared to the NARMA-L2-PSS and LMNN-PSS.

4. Finally it has been concluded that simultaneous application of ANFIS-TCSC with ANFIS-PSS produced good damping characteristics under all operating conditions and disturbances in power system.